

DETERMINATION OF DIFFUSION COEFFICIENTS OF
DILUTE AQUEOUS POLYACRYLAMIDE SOLUTIONS BY
LIGHT BEATING SPECTROSCOPY

Thesis for the Degree of M. S.

MICHIGAN STATE UNIVERSITY

WILLIAM D. STUTESMAN

1972

674 218

ABSTRACT

DETERMINATION OF DIFFUSION COEFFICIENTS OF DILUTE AQUEOUS POLYACRYLAMIDE SOLUTIONS BY LIGHT BEATING SPECTROSCOPY

By

William D. Stutesman

The diffusion coefficient of dilute solutions of a high molecular weight polydisperse sample of polyacrylamide in water was measured as a function of concentration and temperature. The measurements were made using a high resolution optical homodyning spectrometer which incorporated a single mode ion laser as a light source.

The diffusivity was found to vary from 1.31×10^{-8} cm^2/sec to 1.84×10^{-8} cm^2/sec for concentrations in the range of 0.50 to 0.05 weight per cent and measured at temperatures between 25°C and 35°C. The temperature variation of diffusivity was slight because the expected change in the diffusivity for the 10°C range studied was small compared to the experimental error of the measurements. The diffusion coefficient was found to decrease with a decrease in solution

William D. Stutesman

concentration at a fixed temperature for the 0.50, 0.20, and 0.10 weight per cent samples. However, a slight increase in diffusivity was always observed for the 0.05 weight per cent solution compared with the 0.10 weight per cent solution.

The theoretical analysis used in this work, based upon treating the polymer molecule in solution as an isolated sphere, appears adequate as a first approximation. Theoretical refinement of the model by treating the polymer chain as a collection of elements in a Gaussian coil seems appropriate for future study.

DETERMINATION OF DIFFUSION COEFFICIENTS
OF DILUTE AQUEOUS POLYACRYLAMIDE SOLUTIONS
BY LIGHT BEATING SPECTROSCOPY

By

William D. Stutesman

A THESIS

Submitted to
Michigan State University
in partial fulfillment of the requirements
for the degree of

MASTER OF SCIENCE

Department of Chemical Engineering

1972

624773

To my parents

ACKNOWLEDGMENTS

The author would like to express deep appreciation to Dr. Robert F. Blanks for his guidance and encouragement. Appreciation is also extended to Dr. J. B. Kinsinger for his valuable advice and the use of his laser homodyne system. Special thanks is given to Dr. James Peters of The Dow Chemical Company for supplying the polyacrylamide and for his many valuable suggestions. The author also wishes to thank other faculty members and fellow students in the Departments of Chemistry and Chemical Engineering for their help.

TABLE OF CONTENTS

	Page
LIST OF TABLES	v
LIST OF FIGURES	vi
INTRODUCTION	1
THEORY	6
EXPERIMENTAL	14
Apparatus	14
Preparation of Samples	16
Procedure	17
Data Reduction	19
DISCUSSION OF RESULTS	22
ERROR ANALYSIS	33
SUMMARY AND RECOMMENDATIONS	39
NOMENCLATURE	41
LIST OF REFERENCES	44
APPENDIX A. Experimental Data	46
APPENDIX B. Alignment of Light Receiving System	50
APPENDIX C. Adjustment of the Scattering Angle	53

LIST OF TABLES

Table	Page
1. The Effect of Temperature and Concentration on the Diffusion Coefficient	23

LIST OF FIGURES

Figure		Page
1.	Comparison of (a) the optical heterodyne method with (b) the optical homodyne (self-beat) method	2
2.	The relation between the power spectrum of the scattered light and the particle distribution in the fluid	10
3.	Block diagram of the homodyning spectrometer . .	15
4.	The effect of concentration on the diffusion coefficient at 25°C	24
5.	The effect of concentration on the diffusion coefficient at 30°C	25
6.	The effect of concentration on the diffusion coefficient at 35°C	26
7.	Spectrum of scattered light from a 0.05% solution at 25°C and 60°. $\Delta\omega = 159$ Hz	28
8.	The effect of the scattering angle on the half-width. Both runs were with 0.05% solution at 35°C	36
9.	Light receiving system, side view	51
10.	Closeup of the homodyne system	54

INTRODUCTION

The first important work with the spectrum of scattered light was done by Forrester^(1,2) in 1947 and 1948 when he proposed that two beams of light with slightly differing frequencies could be mixed (heterodyned) resulting in a beat note which could be detected in a nonlinear detector. This concept did not result in any useful applications until the modern laser was developed. With the laser's extremely narrow line width of a few Hz or less, it is possible to detect a frequency shift as small as 10 Hz. This level of sensitivity makes it possible to experimentally study the thermodynamic variables that constantly fluctuate about mean values and which describe a system of many particles. Such phenomena as the fluctuations of the dielectric constant of a solution caused by Brownian motion of solute molecules in solution can thus be measured.

The first experimental application of the principle of light beating was done by Cummins, Knable, and Yeh⁽³⁾ who developed an optical heterodyne technique shown in Figure 1(a). The scattered beam from the solution and the unbroadened beam

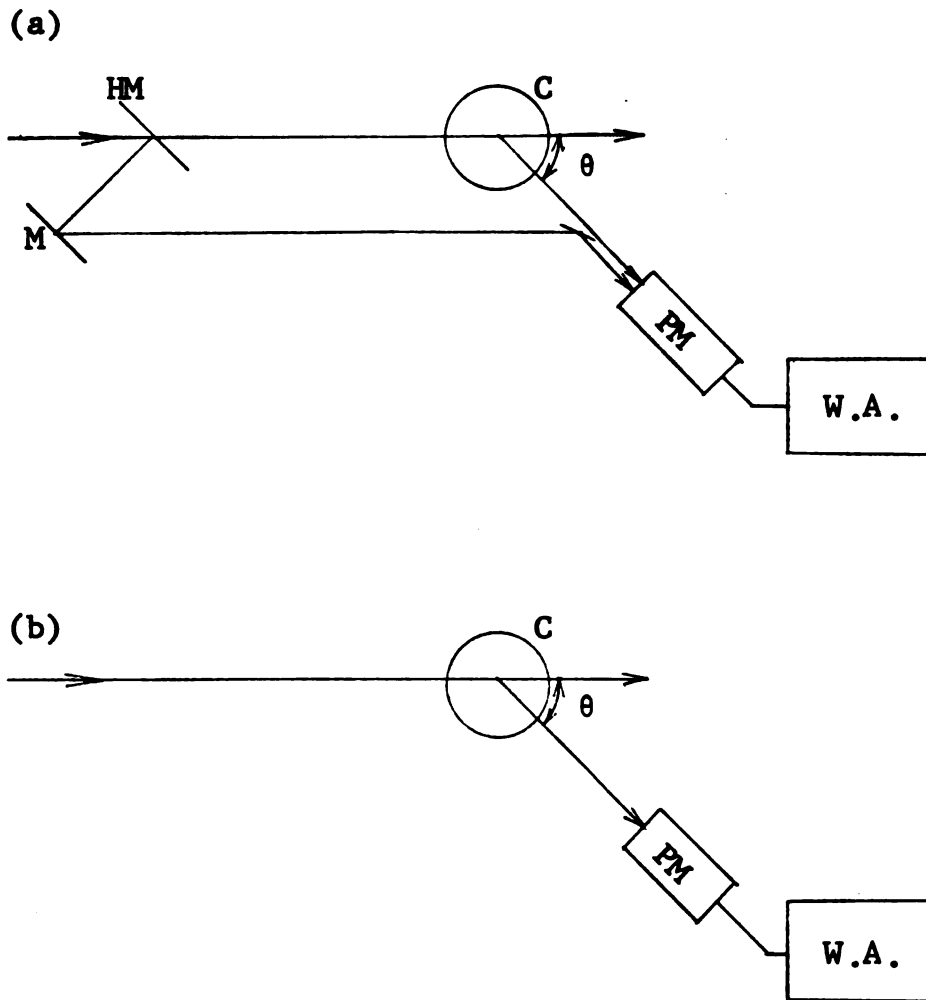


Figure 1.--Comparison of (a) the optical heterodyne method with (b) the optical homodyne (self-beat) method

HM = Half mirror
M = Mirror
C = Cell
PM = Photomultiplier tube
W.A. = Wave analyzer

from the laser follow parallel paths to the surface of the photomultiplier tube. The beating effect then takes place between the unshifted beam and the scattered beam.

Later, the optical self-beat method shown in Figure 1(b) was developed. The scattered light reflected on the photomultiplier has a frequency distribution. The components of this spectrum beat with each other causing fluctuations in the output of the photomultiplier tube which can be analyzed by the wave analyzer. The self-beat spectrometer is superior to the heterodyne system in that it is much simpler and it does not detect any uniform motion of the solution. Therefore, it is relatively insensitive to convective currents.

These light beating systems have already been used for many applications such as measuring the translational diffusion coefficient of monodisperse polystyrene spheres in dilute solutions^(4,5,6), measurements on biological macromolecules^(5,6,8), and polystyrene solutions^(7,9). The spectrum of light scattered from pure fluids and solutions near their critical points has also been measured^(10,11).

In a series of recent papers, Pecora has developed theories predicting the analytical form of the spectrum of light scattered from rods, once-broken rods, flexible-coil macromolecules in the free draining approximation of the

pear-necklace model, and Gaussian coils⁽¹²⁻¹⁸⁾. For a free draining, monodisperse Gaussian coil Pecora showed⁽¹²⁾ that the spectral distribution of the scattered light is given by

$$S_{\infty}(K, \omega) = P_{0\infty}(x) (1/2\pi) (2K^2D / [\omega^2 + (K^2D)^2]) \\ + \sum_{\substack{\text{even} \\ j=2}}^{\infty} P_{1\infty}(x, j) \left(\frac{1}{2\pi}\right) \frac{2(K^2D + \tau_j^{-1})}{\omega^2 + (K^2D + \tau_j^{-1})^2} + \dots$$

$P_{0\infty}, P_{1\infty}$ = integrated intensities

τ_j = relaxation time of the j th molecular normal mode

K = magnitude of the scattering angle

ω = frequency of the scattered light

D = translational diffusion coefficient

$x = \frac{K^2nb^2}{6}$ = dimensionless scattering parameter

n = degree of polymerization

b^2 = mean squared length of a statistical segment

The first term of this expression is the pure translational term which is the only term present in the analogous expression for solid spherical molecules. The second term, which is related to the intramolecular motion of the molecule, is insignificant at low scattering angles. The accuracy of the

expression above has not yet been tested experimentally with macromolecules in solution.

The purpose of the investigation was to evaluate the use of the laser self-beat spectrometer by measuring the translational diffusion coefficient of dilute solutions of high molecular weight polyacrylamide polymer in water. The only previous work of this kind^(7,9) with the diffusivity of polymer solutions had been done using low to medium molecular weight polystyrene, having a relatively narrow molecular weight distribution. This study used a commercial polymer with a very broad molecular weight distribution and a weight average molecular weight of 9,500,000.

THEORY

When a beam of monochromatic light is passed through a transparent medium, some of the light is scattered because of nonuniformities in the density of the medium (Rayleigh scattering). If these inhomogenities were static, there would be no shift in the frequency of the scattered light. However, in solutions these nonuniformities are due to time dependent random molecular motions which produce local fluctuations in the dielectric constant. Therefore, the frequency of the light scattered by these fluctuations exhibits a spectrum characteristic of the time dependence of the fluctuations. This broadening of the frequency is known as a Doppler shift.

In a laser homodyne, or self-beat spectrometer, the scattered light is focused upon the surface of a photomultiplier tube. See Figure 1. The fluctuations in the resulting photocurrent are proportional to the square of the fluctuations in the incident field. The spectrum of these fluctuations, $I_2(\omega)$, is analyzed by the wave analyzer whose output will be referred to as $[I_2(\omega)]_{out}$. The time dependence

of the electric field of the light reaching the phototube has the form⁽¹¹⁾

$$\bar{E}(t) = \delta\bar{E}(t)e^{-i\omega_0 t}$$

ω_0 = angular frequency of the incident light wave

$\bar{E}(t)$ = incident electric field

The amplitude, $\delta\bar{E}(t)$ is directly proportional to the fluctuations in the dielectric constant of the scattering medium.

The exact nature of this amplitude may be analyzed by continuum theory⁽¹⁰⁾. The scattering sample is considered as a collection of many small, independent volume elements. Each element contains many molecules but is small compared to the wavelength of light. Each single volume element is considered as a small particle with a different dielectric constant than the surrounding medium. A fluctuation in the number of molecules in a volume element will cause a fluctuation in the dielectric constant.

The incident light induces an oscillating dipole moment into each volume element which reradiates light with the spatial distribution of a dipole antenna. The electric field of the scattered light is the sum of the contributions

from each volume element. Einstein derived the following expression for the electric field:

$$\delta\bar{E}(t) = -\bar{E}_0 \frac{\pi \sin \psi}{\lambda^2 R} \exp[i(\bar{K}_s \cdot \bar{R} - \omega_0 t)] (2\pi)^{3/2} (\epsilon - \tilde{\epsilon}(t))$$

\bar{E}_0 = original electric field of the light source

λ = wavelength of the light source

ω_0 = frequency of the light source

\bar{K}_s = wave vector of the scattered light

ψ = angle between the polarization of the original electric field and \bar{K}_s

$(\epsilon - \tilde{\epsilon}(t))$ = fluctuating value of the dielectric constant

\bar{R} = distance from observer to the scattering center

The spectrum of the scattered light, above, will now be related to the autocorrelation of the electric field, $R(\tau)$. This autocorrelation function is the time average of the product of the signal, at any time t , with the signal at any time $t + \tau$.

$$R_1(\tau) = \langle \bar{E}(t) \cdot \bar{E}^*(t+\tau) \rangle = \langle \delta\bar{E}(t) \delta\bar{E}^*(t+\tau) \rangle e^{-i\omega_0 \tau}$$

The Wiener-Kintchine theorem can be used to obtain the spectral power density from the autocorrelation function. This

theorem states⁽¹⁹⁾ that the power spectrum, $I_1(\omega)$, of a random signal is the Fourier transform of the autocorrelation function.

$$I_1(\omega) = \frac{1}{2\pi R_1(0)} \int_{-\infty}^{\infty} R_1(\tau) e^{i\omega\tau} d\tau$$

$I_1(\omega)$ = power spectrum of the scattered light falling on the photomultiplier tube

The spectra is normalized by:

$$\int_{-\infty}^{\infty} I_1(\omega) d\omega = 1$$

The above derivation is summarized in Figure 2.

The photocurrent is proportional to $|\bar{E}(t)|^2 = |\delta\bar{E}(t)|^2$. This quantity contains both a dc contribution, which is experimentally blocked before analysis of the spectrum, and a fluctuating part whose autocorrelation function, $R_2(\tau)$, is the square of the correlation function for $\delta\bar{E}$ ⁽¹¹⁾.

$$R_2(\tau) = |R_1(\tau)|^2$$

The spectrum $I_2(\omega)$ of the fluctuations in $|\delta\bar{E}(t)|^2$ is thus related to the square of the correlation function for the scattered field:

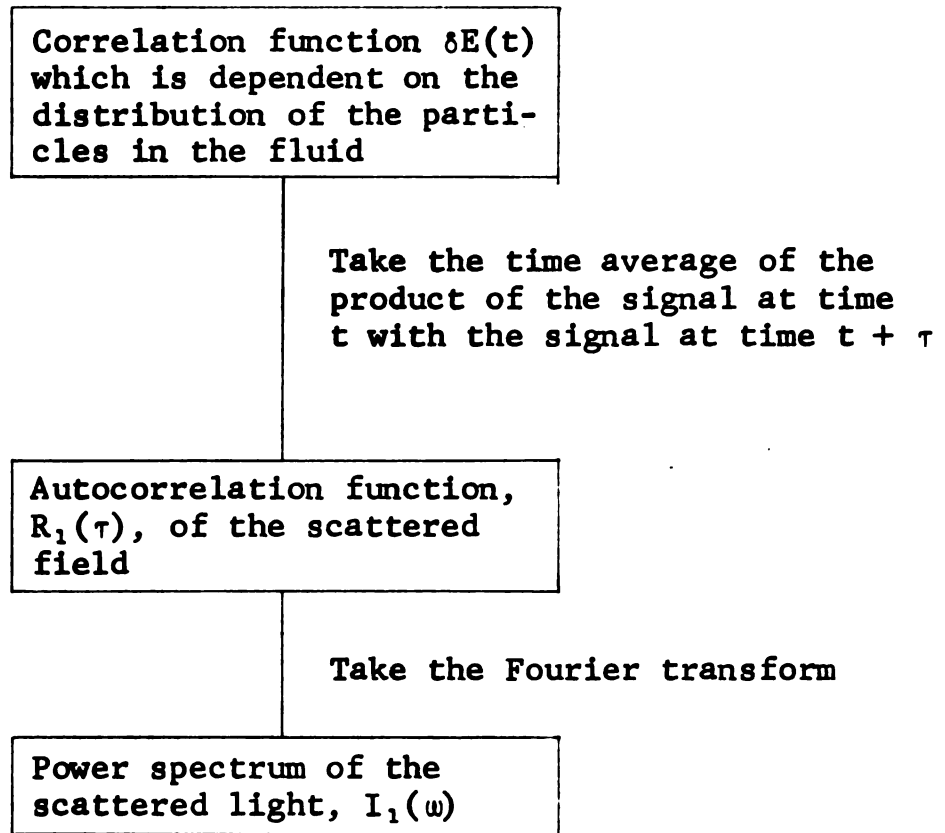


Figure 2.--The relation between the power spectrum of the scattered light and the particle distribution in the fluid

$$I_2(\omega) = \frac{1}{2\pi |R_1(0)|^2} \int_{-\infty}^{\infty} |R_1(\tau)|^2 e^{i\omega\tau} d\tau$$

$I_2(\omega)$ can be related directly to $I_1(\omega)$ by the following expression:

$$I_2(\omega) = \int_{-\infty}^{\infty} I_1(\omega') I_1(\omega' - \omega) d\omega'$$

This relationship expresses the spectral density at ω as the sum total of all the beat notes between spectral components separated an amount ω apart.

If the correlation function for the scattered field decays exponentially with a decay rate Γ such as

$$R_1(\tau) = \langle |\delta E(t)|^2 \rangle e^{-i\omega_0 \tau} e^{-\Gamma\tau}$$

then the power spectrum $I_1(\omega)$ is a Lorentzian shaped line centered at ω_0 with half width Γ . The spectrum $I_2(\omega)$ is also a Lorentzian shaped line centered at $\omega = 0$ with a half width at half the maximum amplitude of 2Γ . Therefore the power spectrum of the photocurrent is represented by

$$I_2(\omega) = \frac{2(\Gamma/2\pi)}{\omega^2 + [2(\frac{\Gamma}{2\pi})]^2}$$

The experimentally measured half width, $\Delta\omega$, is $\frac{\Gamma}{\pi}$ cycles per second.

The decay rate, Γ , can now be related to the translational diffusion coefficient by the continuum theory of scattering. This approach assumes that the concentration fluctuations follow Fick's second law of diffusion,

$$\frac{\partial}{\partial t}[\delta C(r, t)] = DV^2[\delta C(r, t)]$$

$\delta C(r, t)$ = concentration fluctuation,
dependent on time and position

D = translational diffusion coefficient

By solving this expression at $t = 0$, it can be shown that, for a fluctuation in concentration with wavelength λ_f , the fluctuation will decay exponentially at a rate

$$\Gamma = D\left(\frac{2\pi}{\lambda_f}\right)^2 = DK^2$$

$$K = \frac{2\pi}{\lambda_f}, \text{ the wave vector}$$

λ_f can be related to the light beam incident on the sample and the scattering angle by Bragg's law,

$$\frac{\lambda}{n} = 2\lambda_f \sin \frac{\theta}{2}$$

λ = wavelength of the incident laser beam

θ = scattering angle

n = refractive index of the sample solution

Γ can now be expressed as

$$\Gamma = D \left[\frac{4\pi n \sin \frac{\theta}{2}}{\lambda_0} \right]^2$$

Solving this expression for D and substituting $\Delta\omega\pi$ for Γ ,

$$D = \frac{\Delta\omega\lambda^2}{16\pi n^2 \sin^2 \frac{\theta}{2}}$$

It can thus be seen that the translational diffusion coefficient of a macromolecule in solution can be determined with a self-beating spectrometer by measuring the half width of the Lorentzian spectra produced at a specific scattering angle. This expression assumes that the half-width of the spectrum is due only to translational diffusion. Pecora has shown⁽¹²⁾ that this broadening is also due to intramolecular motion for macromolecules. However, this contribution is quite small at low scattering angles.

EXPERIMENTAL

Apparatus

The experimental measurements were made with a system known as a laser "self-beat" or homodyne spectrometer. This system consisted of four parts: a laser light source, the scattering cell, light collecting optics, and an electronic wave analyzer. This is shown schematically in Figure 3. The laser was a Spectra Physics Model 165 ion laser. It operated with a single mode at 5145 \AA and was capable of a maximum output of 750 mW. The light beam from the laser was then directed through the center of the cylindrical sample cell which was mounted in a temperature control cell. This temperature control cell utilized electric heating elements and a proportional controller to hold the temperature of the sample solution constant within a few hundredths of a degree Centigrade. The scattering angle was changed by redirecting the incident beam with a mirror. All scattering angles from 0° to 180° were made possible by rotation and translation of the mirror on its moveable mount.

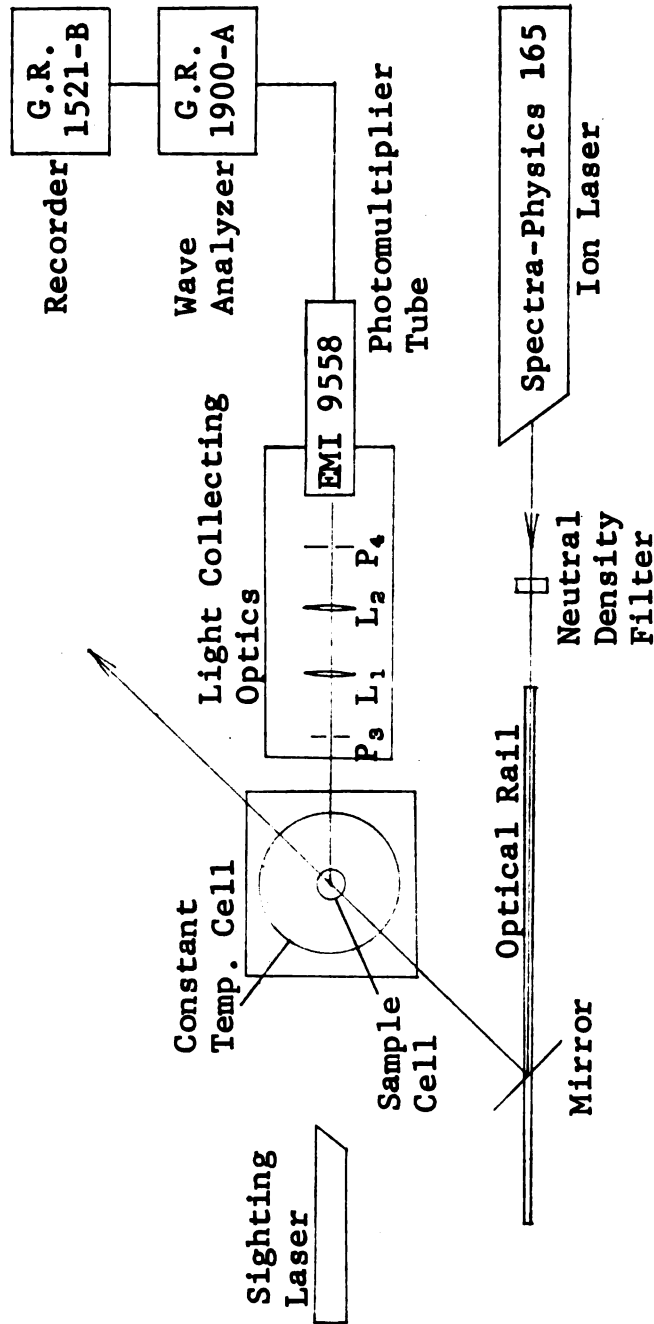


Figure 3.--Block diagram of the homodyning spectrometer

P₃, P₄ = Pinholes
 L₁, L₂ = Lenses

The scattered light was collected by a series of lenses and pinholes and focused upon the surface of the EMI 9558 photomultiplier tube. This photomultiplier was chosen because of its high gain, low noise, and optimum quantum efficiency at the laser frequency.

The spectrum of the resulting photocurrent was obtained with a General Radio 1900-A wave analyzer and a General Radio 1521-B graphic level recorder. The wave analyzer had an internal calibration that was used before each measurement. This system produced continuous, convenient records of the frequency spectra.

The entire system was mounted on a vibration-free table located in a basement laboratory. As a result, building vibrations were not found to be a problem.

Preparation of Samples

The solutions of polyacrylamide were made by diluting a 1.00% (by weight) stock solution with measured aliquots of water. The polymer was a polydisperse sample of the commercial type manufactured by The Dow Chemical Company. It had a weight average molecular weight of 9,500,000, measured by light scattering. The sample contained a low molecular weight

stabilizer which was extracted by washing the sample several times with an 80% solution of acetone in water. The liquid was then decanted off and the polymer dried under a vacuum. The final polymer solutions and the original stock solution were made with water which was first distilled, deionized, and then distilled again in a glass distillation column.

Next, the solutions were purified by centrifuging them at 30,000-50,000 G for two hours. The sample cells were then filled by carefully siphoning the purified solutions from the upper third of each centrifuge tube. The solutions in the sample cells were then degassed by successive freezing and applications of vacuum. Then, the cells were sealed with a glass cutting torch. It was hoped that this procedure would eliminate, or at least minimize, degradation of the samples with time.

Procedure

A careful alignment of the laser homodyning system was necessary before measurements could be made. The beam from a small "sighting" laser (shown in Figure 1) was aimed into the light receiving system. It was then possible to adjust the pinholes and lenses so that they defined a straight

optical path. The path of the main ion laser beam was then adjusted so the desired scattering angle could be measured (see Appendix C for details). Next, the cylindrical sample cell was mounted in the temperature control cell which was placed so the incident laser beam passed directly through the center of the sample cell.

The sample solution was allowed to remain in the temperature control cell for an hour before any measurements were made, to insure that complete thermal equilibrium was reached. Since all of the measurements were made within 10°C of room temperature, it did not take long to reach this equilibrium. During this time period, the laser and the wave analyzer were left on to insure that their operation would be stable during the experimental measurements.

After the complete system was aligned and ready, the measurements were then made with the room lights turned off to prevent stray light entering the system. The power supply to the laser was always adjusted to 200-300 mW where the operation of the laser was most stable. This was much more light than was required, so the intensity of the beam was reduced by placing neutral density filters in the path of the incident beam. Very dilute solutions scatter much less light

than concentrated solutions so a more intense incident beam was used for these dilute samples. This was accomplished by using a neutral density filter with a higher light transmittance.

The wave analyzer was always calibrated before each experimental run to insure an accurate, reproduceable analysis. All measurements were recorded with a 10 cycle bandwidth and the slowest chart speed and writing speed available. The effect of these conditions was to average out much of the random noise fluctuations in the spectra.

A single run consisted of measuring the spectra of a sample at a fixed temperature and scattering angle. All of the solutions were measured at scattering angles of 38°, 50°, and 60° at temperatures of 25°C, 30°C, and 35°C. Samples of 0.50%, 0.20%, 0.10%, and 0.05% (by weight) polyacrylamide in water were used.

Data Reduction

The spectrum at a fixed temperature and scattering angle, analyzed by the wave analyzer was recorded on chart paper by the recorder logarithmically, in decibels. Therefore, the output of the wave analyzer, $[I_2(\omega)]_{\text{out}}$ was related to the recorder output by,

$$[I_2(\omega)]_{\text{out}} = \exp\left[\frac{2.3A(\omega)}{20}\right]$$

$A(\omega)$ = amplitude of the signal at a given frequency, in decibels, plotted by the recorder

For the G. R. 1900 wave analyzer, the output $[I_2(\omega)]_{\text{out}}$ is actually the square root of $I_2(\omega)$. This quantity, which is the desired spectrum of the photocurrent fluctuation, can now be expressed in terms of the recorder output:

$$I_2(\omega) = [I_2(\omega)]_{\text{out}}^2 = \exp\left[\frac{2.3A(\omega)}{10}\right]$$

Data points were then taken from the recorded spectra at 30 Hz intervals and exponentiated in the above manner so that the data was in the form $(I_2(\omega_i), \omega_i)$. The characteristic Lorentzian was found by plotting $1/I_2(\omega_i)$ against ω_i^2 . Such a plot is linear when the spectrum is Lorentzian. The best straight line was then fit to these points by a computer fit, Kinfit, which was developed by the Department of Chemistry at Michigan State University. The resulting slope and intercept were then used to calculate the half width at half the maximum amplitude, $\Delta\omega$, of the Lorentzian which best fit the data. Then, the translational diffusion coefficient for each run was calculated by the following relationship:

$$D = \frac{\Delta\omega\lambda^2}{16\pi n^2 (\sin\frac{\theta}{2})^2}$$

which was derived earlier. The refractive index, n , of each sample solution, at each temperature, was measured experimentally. The wavelength of the laser beam was 5145 Å. The experimental diffusion coefficient for each sample at a given temperature was obtained by averaging the coefficients obtained from all the scattering angles.

DISCUSSION OF RESULTS

The diffusion coefficients of the 0.50%, 0.20%, 0.10%, and 0.05% (by weight) polyacrylamide samples measured at 25°C, 30°C, and 35°C are tabulated in Table 1. Each value was calculated by averaging the data obtained at all the scattering angles for that particular solution and temperature. The same information is shown graphically in Figures 4, 5, and 6. It can be seen that the values of the diffusion coefficient range from 1.31×10^{-8} to $1.84 \times 10^{-8} \frac{\text{cm}^2}{\text{sec}}$. These values may be compared to the work done by Sholtan⁽²⁰⁾ who found the relationship,

$$D = 8.46 \times 10^{-4} M^{-.69}$$

M = molecular weight

to be accurate for monodisperse samples of polyacrylamide in water with molecular weights from 19,400 to 534,000. Of course, this relation does not take into account the effect of concentration on the diffusion coefficient. Applying this equation to a polymer with a molecular weight of 9,500,000, a diffusion coefficient of $1.30 \times 10^{-8} \frac{\text{cm}^2}{\text{sec}}$ is predicted.

Table I

The Effect of Temperature and Concentration
on the Diffusion Coefficient

Concentration % by Wt.	$D \times 10^8 \frac{\text{cm}^2}{\text{sec}}$		
	25°C	30°C	35°C
0.50	1.84	1.84	1.82
0.20	1.53	1.59	1.64
0.10	1.40	1.31	1.39
0.05	1.70	1.33	1.47

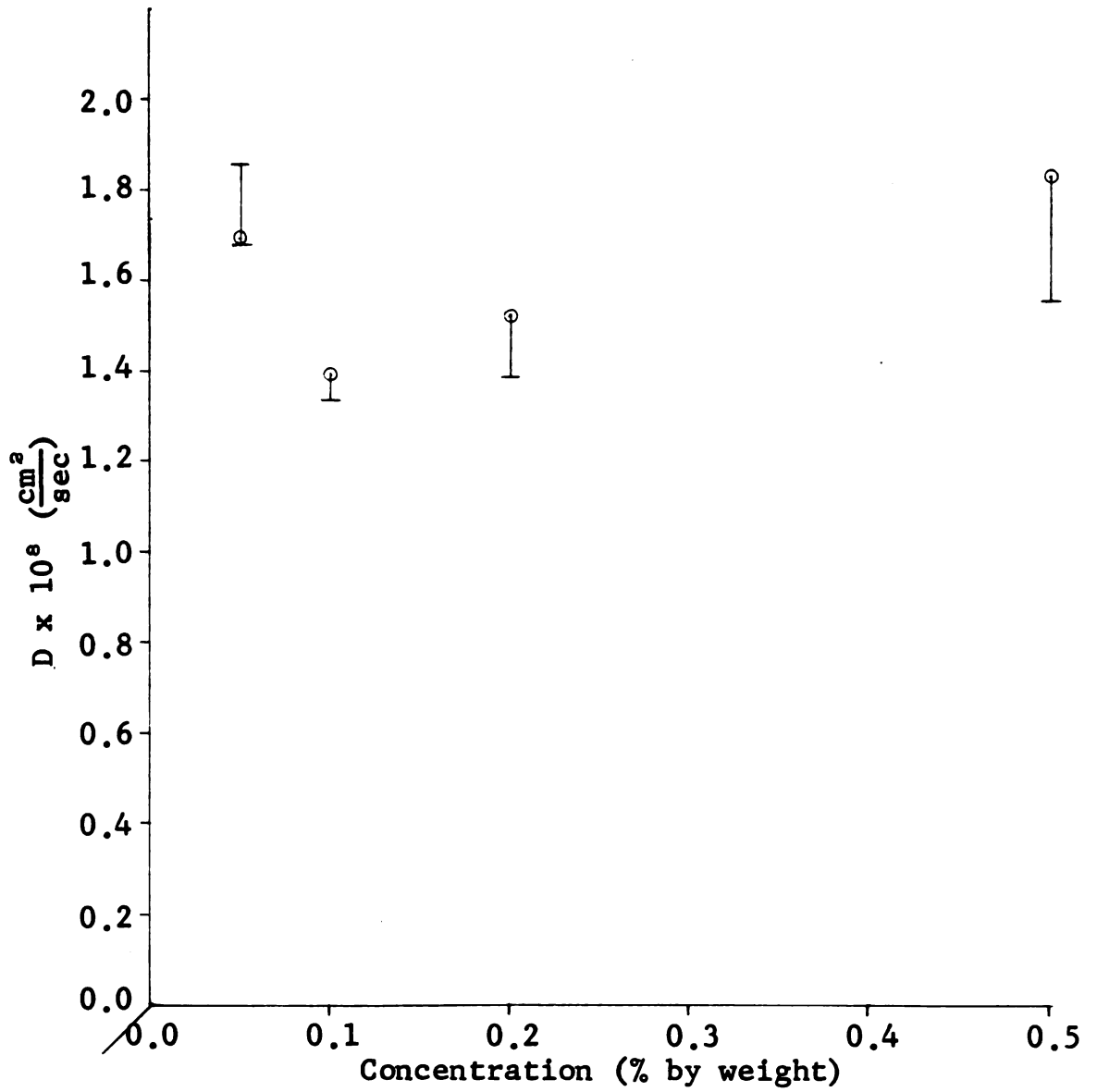
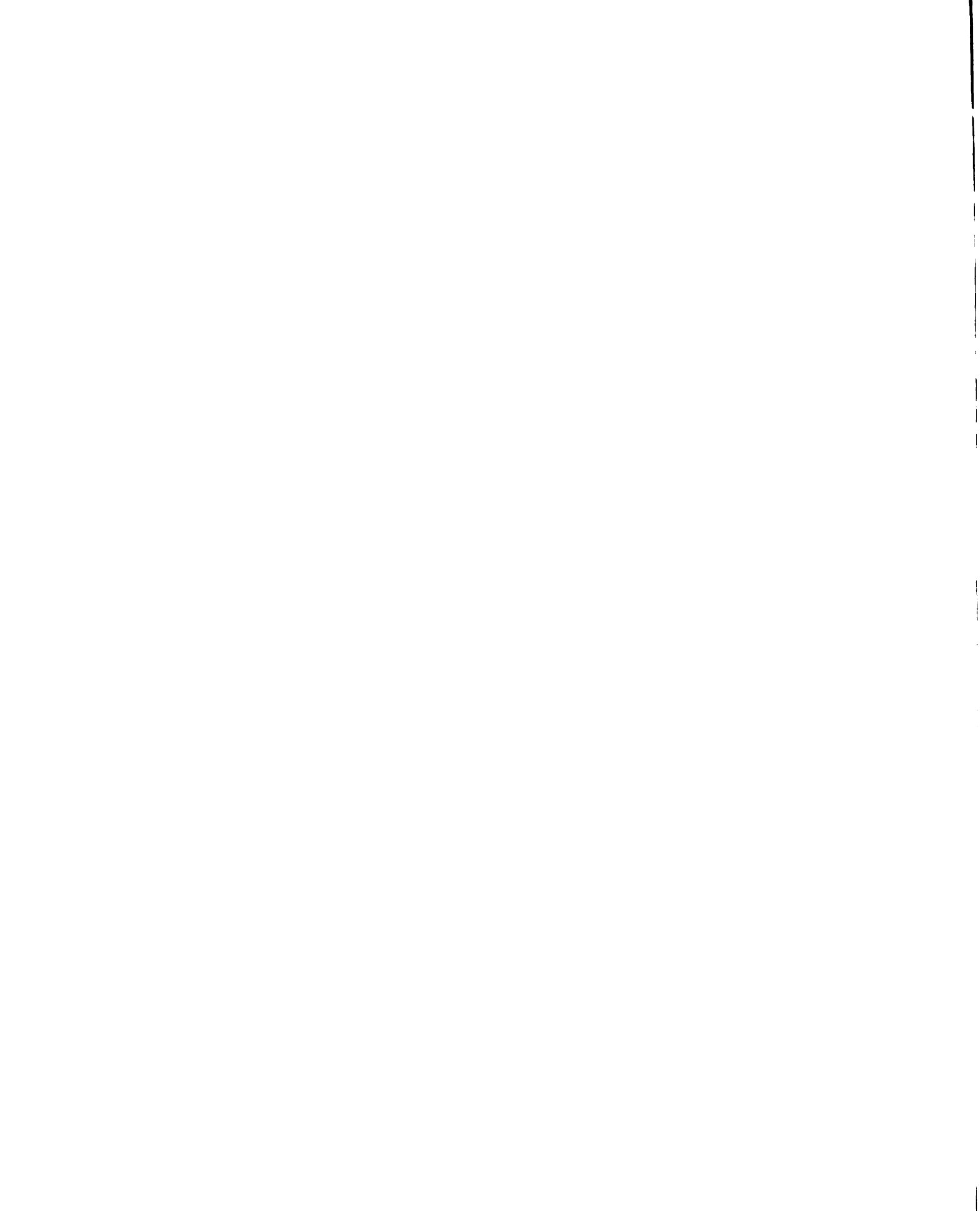


Figure 4.--The effect of concentration on the diffusion coefficient at 25°C.



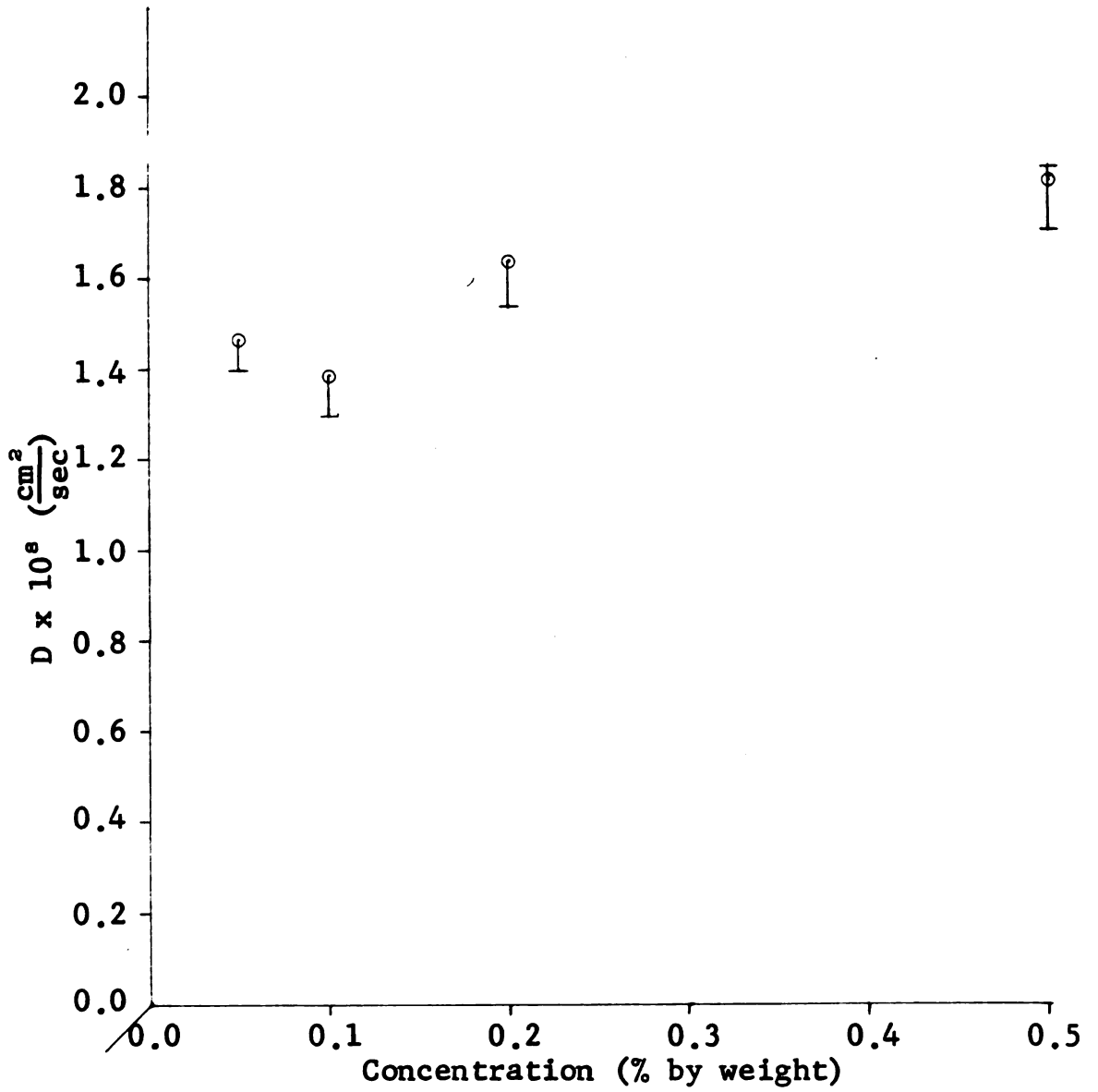


Figure 5.--The effect of concentration on the diffusion coefficient at 30°C.

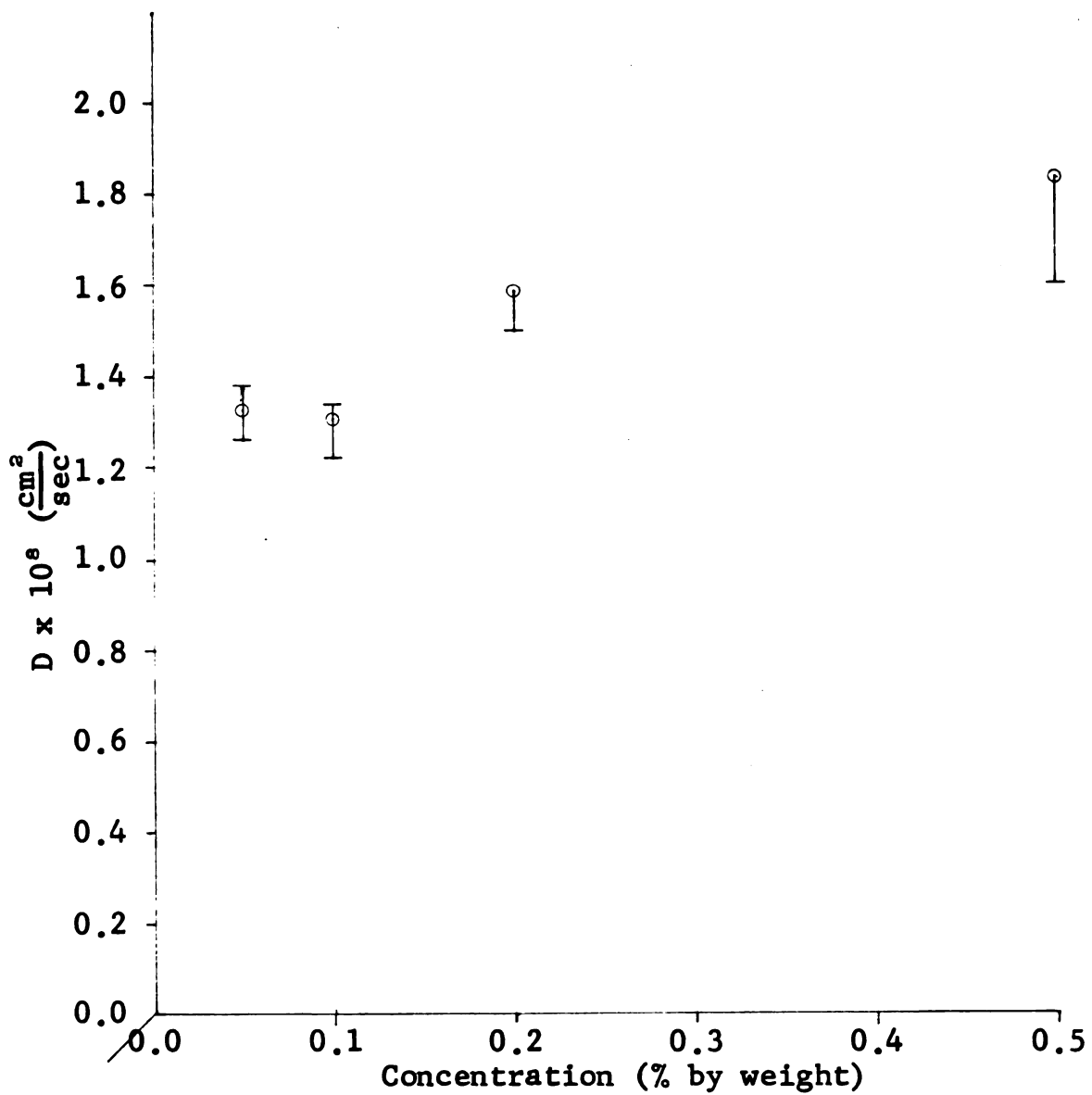


Figure 6.--The effect of concentration on the diffusion coefficient at 35°C.

This is in good agreement with the experimental results when one considers that the molecular weight of the sample was much greater than those used in the development of Sholtan's relationship, and also that the molecular weight distribution of the polyacrylamide used in this study was very broad while Sholtan's work was done with monodisperse samples. It must be noted that although the experimental spectrum of a polydisperse sample may appear to be nearly Lorentzian in form, the diffusion coefficient calculated from this spectrum has no obvious relation to the coefficient of any particular species in the distribution. In other words, the diffusion coefficient for a polydisperse sample with a weight average molecular weight of 9,500,000 can not be expected to be the same as that of the particular species with that molecular weight. The measured diffusion coefficient for such a polydisperse sample is an average coefficient weighted by the individual species that form the distribution.

It can be seen in Figure 7 that the spectrum of the scattered light is not perfectly Lorentzian. This may be partially accounted for by experimental error. However, it is very likely that it is also caused by the effect of intramolecular motion. Pecora has suggested⁽¹²⁾ that the spectrum

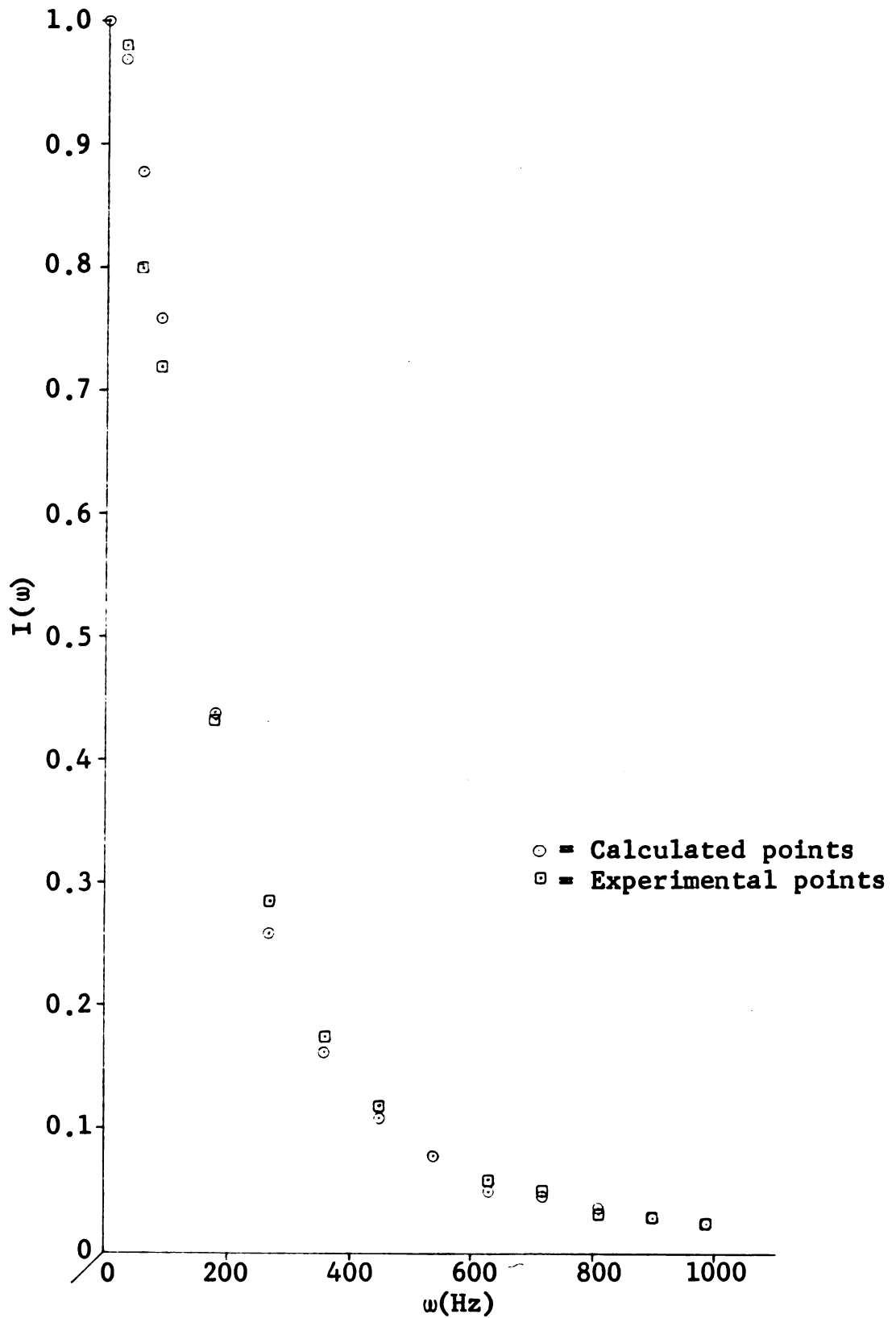


Figure 7.--Spectrum of scattered light from a 0.05% solution at 25°C and 60°. $\Delta\omega = 159$ Hz

of scattered light is due to the summation of two terms: a term attributed to purely translational diffusion which is Lorentzian in nature, and a term caused by intramolecular motion which is non-Lorentzian. Therefore, deviations of the spectra from Lorentzian form may be explained by the presence of these intramolecular effects. Thus, the translational diffusion coefficients were calculated from experimental line widths that might not have been caused strictly by translational effects.

It was hoped at the beginning of this study that it would be possible to examine the effect of temperature on the diffusion coefficient. However, this did not prove to be feasible because the temperature range studied was so narrow that the effect of the change in temperature was small compared to the experimental error. This can be seen in Table 1. The range of temperatures for this study was from 298°K to 308°K. If the temperature dependence predicted by the Stokes-Einstein equation ($D = kT/6\pi\eta r$), originally developed for spheres, is used as an approximation, then the effect of this 10°K temperature change on the diffusivity could only be expected to cause about a 3% difference. This is less than the experimental error.

The temperature range was limited by experimental considerations. Because the bulk of the measurements were made during the humid summer months, lowering the temperature of the samples below room temperature would have resulted in condensation on the outside of the sample cell, which would have affected the light scattering. Therefore, a lower bound on the temperature of 25°C was set. The maximum temperature used was 35°C. It was feared that degradation of the samples might be a problem at higher temperatures.

The effect of concentration on the diffusion coefficient for each temperature is shown in Figures 4, 5, and 6. These plots show that the diffusivity decreases with decreasing solution concentration to a minimum at 0.1 wt. %. Then, there is an increase in the coefficient at 0.05 wt. %. This sudden inflection is difficult to account for and makes it hard to develop a general relationship between diffusivity and concentration. Without this general relationship it is impossible to extrapolate to zero concentration to find the diffusion coefficient there. This inflection has been noted by experimentalists working with other solute-solvent systems (8,21,22).

Diffusivity-concentration data is often difficult to interpret because of the way the nonideality of the solution changes with concentration. The variation in the diffusion coefficient will be caused by both thermodynamic and hydrodynamic effects⁽²³⁾. The diffusion coefficient can be related to the frictional coefficient, the concentration, and the activity coefficient of the solution by:

$$D = \frac{kT}{f} \left(1 + \frac{\partial \ln \gamma_i}{\partial \ln c_i} \right)$$

γ_i = activity coefficient

c_i = concentration

f = frictional coefficient

k = Boltzmann's constant

For a polymer in any solvent better than a θ -solvent, the solution will exhibit a negative deviation from ideality, $\frac{\partial \ln \gamma_i}{\partial \ln c_i}$ will be positive, and this factor will tend to increase the diffusion coefficient as the solution concentration increases. The equation above is based on the assumption that the hydrodynamic resistance to the motion of a particle is independent of the presence of other similar particles. This is a good assumption only if the diffusing particles are far apart. At higher concentrations, the hydrodynamic disturbances created by their motion will interact causing a

change in the frictional coefficient. In general, an increase in concentration will cause an increase in the frictional coefficient which will, in turn, decrease the diffusivity. Therefore, the thermodynamic and hydrodynamic effects become more important as the concentration increases. However, they affect the diffusion coefficient in opposite directions. The change in their relative effects as the concentration changes could explain the inflection in the plotted curves described above.

ERROR ANALYSIS

The errors in the experimental data may be attributed to three main factors:

1. Sample preparation
2. System limitations
3. Data analysis

The preparation of the samples was a difficult task. Dissolving the polyacrylamide in water was a very slow process. While the stock solution was being prepared, water continually evaporated although every possible precaution was taken to prevent this. This meant that the concentration of the stock solution was not known with complete certainty. The actual samples were made by diluting the stock solution by weight. Therefore, the uncertainty in the value of the stock solution concentration was also present in the sample solutions. However, the relative concentrations of the samples was known very precisely because it was possible to dilute the stock solution very accurately. Perhaps the most

critical step in the preparation of the samples was their purification. It was absolutely necessary to remove all of the dust and other impurities from the solutions, as they represented very effective light scatterers. Their presence in the sample would tend to increase the half-width of a spectra. Many experimenters have attempted to remove such impurities with millipore filters. However, the solutions used in this study were too viscous for such filtration and it was feared that any attempts to improve their filtering characteristics - by heating or application of pressure - would result in degradation of the polymer. Therefore, the use of the purest available water for the solutions and the method of centrifugation of the final samples were felt to be the best purification techniques.

The alignment and operation of the light beating system was a very critical parameter. Lining up the incident beam so that the scattering angle was known precisely, centering the sample cell directly in the beam, proper temperature control, and good alignment of the receiving optics were all necessary to minimize the error in the data. One source of experimental error that could not be minimized with the system used was the fluctuating output of the chart

recorder. This random noise made it difficult to find the exact amplitude at each frequency in the spectra.

The effect of these system errors is illustrated in Figure 8, which shows the results of two experimental runs made with the same sample solution at the same temperature. The theory, discussed earlier, predicts that a plot of spectral half-width ($\Delta\omega$) versus $(\sin \frac{\theta}{2})^2$ will be linear with an intercept at the origin. It can be seen that the data from Run #2 is quite linear, while the data from Run #1 is not. The deviations in the results of Run #1 must be accounted for by system errors, since all the other details of Run #1 and Run #2 were identical, including the method of data analysis that was used. Whenever duplicate runs were made, the linearity of the results was used as the criteria in deciding which data to use.

Another source of error was in the data reduction. The spectra shown in Figure 7 was calculated in the following manner: The reciprocal of the amplitude $1/I_2(\omega_1)$ was plotted versus ω_1^2 . The slope and intercept of the line fitted to this data was then used to calculate the characteristic maximum amplitude and half-width of the Lorentzian that fit the data. Figure 7 is a normalized spectra (a spectra with a

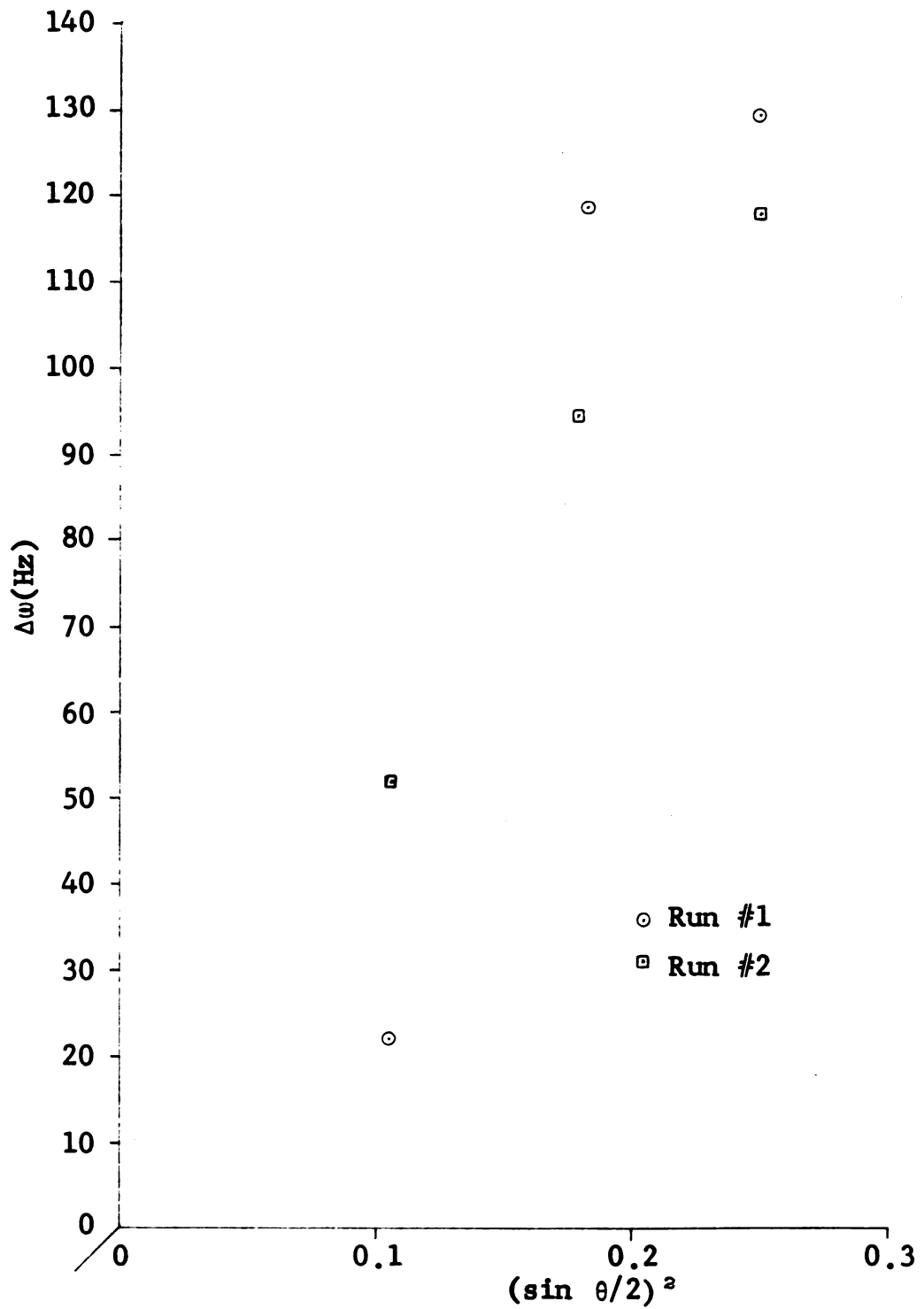


Figure 8.--The effect of the scattering angle on the half-width. Both runs were with 0.05% solution at 35°C.

maximum amplitude of one at zero frequency) which makes it possible to compare the experimental spectrum with the calculated Lorentzian. Another approach that was tried was fitting the experimental data directly to the equation of the Lorentzian, $I_2(\omega) = \frac{\Delta\omega}{\omega^2 + (\Delta\omega)^2}$. However, it was possible to see, by comparing normalized spectra such as Figure 7, that the computer fit was closer with the linear plot.

Figure 7 also shows that the worst fit was at the low frequency end of the spectrum. This could have been corrected by weighting these points more heavily during the analysis. However, there was no apparent reason to believe that these points were more important than the higher frequency points. Therefore, in the actual analysis all the points were weighted equally.

The major uncertainty in the data analysis was in the method used to find the average diffusion coefficient once the spectral half-width was found at each scattering angle. Four different methods were used to calculate the diffusivity. Method 1 involved calculating the half-width at each angle with the linear fit described above. The diffusion coefficients were calculated for each scattering angle and then arithmetically averaged to get the mean diffusivity.

Method 2 also used a computer line-fit to find each spectral half-width. Then a plot of $\Delta\omega$ versus $(\sin \theta/2)^2$, as in Figure 5, was made. The slope of the best straight line through the data points and the origin then represented an average value of $\Delta\omega/(\sin \theta/2)^2$. The average diffusion coefficient was then calculated by the following relationship:

$$D = \frac{\lambda^2}{16\pi^2} \left(\frac{\Delta\omega}{(\sin \theta/2)^2} \right) = \frac{\lambda^2}{16\pi^2} (\text{slope})$$

Method 3 and Method 4 were exactly like Method 1 and Method 2, respectively, except that the half-width of each spectrum was found by fitting the data directly to the equation of the Lorentzian in the manner described earlier. Figures 4, 5, and 6 show the effect the method of analysis has on the final results. The center point at each concentration was calculated by Method 1. The error bars were calculated by plotting the results of Methods 2, 3, and 4, which were used on the very same raw data that was analyzed by Method 1.

The per cent uncertainty in the diffusivity due to the method of data analysis can be calculated by

$$\% \text{ Uncertainty} = \frac{D_{\text{Method 1}} - D}{D_{\text{Method 1}}} \times 100\%$$

This was found to vary from 4.28% to 15.2%.

SUMMARY AND RECOMMENDATIONS

Light beating spectroscopy was found to be a fast, convenient method of measuring diffusion coefficients in macromolecular solutions. It was felt that the results of this study were quite accurate but that there is a potential for much greater precision with this technique. The system itself could be greatly improved by refining the procedure for aligning the sample cell and the receiving optics. As it was mentioned earlier, these alignments are extremely critical. Placing an additional pinhole between the two lenses in the light receiving system at their common focal point (see Figure 9) would prevent stray light from reaching the photomultiplier tube. The problem of reading the average amplitudes from the fluctuating output of the chart recorder could be eliminated by connecting an on-line digital computer directly into the wave analyzer. Such a computer could scan the entire spectrum hundreds of times in a matter of minutes to provide time smoothed data. This would greatly improve the precision of the data and speed up the analysis.

Figure 8, for example, shows that the data is not completely Lorentzian. This could be due to experimental error and poor analysis. However, it could be the result of the polydispersity of the sample. An investigation of this possibility would be an interesting study. It could be approached experimentally by working with both monodispersed and polydispersed samples. It would also be interesting to fit the data from the polydispersed sample with multiple Lorentzians, each representing a species of the molecular weight distribution.

NOMENCLATURE

NOMENCLATURE

$A(\omega)$	Amplitude of the signal, read from the chart recorder
c_i	Concentration
$\delta c(r, t)$	Concentration fluctuation
D	Translational diffusion coefficient
\bar{E}_0	Original electric field of the light source
$\bar{E}(t)$	Electric field of the light incident on the photomultiplier tube
$\delta \bar{E}(t)$	Amplitude of the electric field
f	Frictional coefficient
$I_1(\omega)$	Spectrum of the light incident on the photomultiplier tube
$I_2(\omega)$	Spectrum of the photocurrent fluctuations
$[I_2(\omega)]_{out}$	Output of the wave analyzer

k	Boltzmann's constant
\bar{K}	Scattering vector
K	Magnitude of the scattering vector
n	Refractive index of the solution
\bar{R}	Distance from observer to the scattering center
$R_1(\tau)$	Autocorrelation function of the electric field incident on the photomultiplier tube
$R_2(\tau)$	Autocorrelation function of the photocurrent fluctuations
t	Time
T	Temperature

Greek Symbols

γ_i	Activity coefficient
Γ	Decay rate of a concentration fluctuation
$(\epsilon - \tilde{\epsilon}(t))$	Fluctuating value of the dielectric constant
θ	Scattering angle

λ	Wavelength of the incident laser beam
ψ	Angle between the polarization of the original electric field and the scattering vector
ω_0	Frequency of the light source
ω	Frequency of the scattered light
$\Delta\omega$	Half-width of the spectrum at half the maximum amplitude
τ	Time

LIST OF REFERENCES

LIST OF REFERENCES

1. A. T. Forrester, W. E. Parkins and E. Gerjuoy, Phys. Rev. 72 (8), 728-729 (1947).
2. A. T. Forrester, E. Gerjuoy and W. E. Parkins, Phys. Rev. 73 (8), 922-923 (1948).
3. H. Z. Cummins, N. Knable and Y. Yeh, Phys. Rev. Lett. 12, 150 (1964).
4. K. Ohbayashi, S. Kagoshima and A. Ikushima, Jap. J. App. Phys. 11 (6), 808 (1972).
5. M. J. French, J. C. Angus and A. G. Walton, Science 163, 345 (1969).
6. S. B. Dubin, J. H. Lunacek and G. B. Benedek, Proc. Nat. Acad. Sci. 57, 1164 (1967).
7. T. F. Reed and J. E. Frederick, Macromolecules 4, 72 (1971).
8. S. Fujime, J. Phys. Soc. Jap. 29, 416 (1970).
9. J. E. Frederick, T. F. Reed and O. Kramer, Macromolecules 4, 242 (1971).
10. J. W. Dunning, Jr., thesis, Case Western Reserve University, Cleveland, Ohio (1967).
11. N. C. Ford, Jr., and G. B. Benedek, Phys. Rev. Lett. 15, 649 (1965).
12. R. Pecora, J. Chem. Phys. 43, 1562 (1965).

13. R. Pecora, *ibid.* 48, 4126 (1968).
14. R. Pecora, *ibid.* 49, 1032 (1968).
15. R. Pecora, *ibid.* 49, 1036 (1968).
16. Y. Tagami and R. Pecora, *ibid.* 51, 3293 (1969).
17. R. Pecora and Y. Tagami, *ibid.* 51, 3298 (1969).
18. R. Pecora, *Macromolecules* 2, 31 (1969).
19. W. W. Harman, "Principles of the Statistical Theory of Communication," McGraw-Hill Book Co., New York, 1963, p. 42.
20. Sholtan, *Die Makromolekular Chemie* 14, 169 (1954).
21. W. J. Moore, "Physical Chemistry," 3d. ed., Prentice-Hall, Inc., Englewood Cliffs, N. J., 342 (1962).
22. V. N. Tsvetkov and S. I. Kleinin, *J. Polym. Sci.* 30, 187 (1958).
23. H. Morawetz, "Macromolecules in Solution," Interscience Publishers, New York, 275 (1965).

APPENDICES

APPENDIX A

Experimental Data

The raw data was analyzed by four different methods. The calculated results may be distinguished by the following subscripts:

- 1 Raw data [$I_2(\omega_1)$, ω_1] fitted to the straight line form of the Lorentzian to get $\Delta\omega_1$ for each scattering angle.
- 2 Raw data [$I_2(\omega_1)$, ω_1] fitted directly to the equation of the Lorentzian to get $\Delta\omega_2$ for each scattering angle.
- 3 D was calculated from $\Delta\omega$ at each scattering angle. These diffusivities were then averaged together.
- 4 $\Delta\omega$ was plotted versus $(\sin \theta/2)^2$. The slope of the best straight line through these points and the origin was used to calculate D.

25°C

Conc. Wt. %	n	θ	$\Delta\omega_1$, Hz	$\Delta\omega_2$, Hz	$D_{1s} \times 10^8$ cm ² /sec	$D_{14} \times 10^8$ cm ² /sec	$D_{2s} \times 10^8$ cm ² /sec	$D_{24} \times 10^8$ cm ² /sec
0.50	1.3365	38°	77.0	73.0	1.84	1.57	1.79	1.56
		50°	109	109				
		60°	133	130				
0.20	1.3357	38°	58.2	59.7	1.53	1.43	1.52	1.39
		50°	92.7	92.2				
		60°	121	116				
0.10	1.3355	38°	48.2	45.3	1.40	1.39	1.35	1.34
		50°	90.8	89.8				
		60°	114	110				
0.05	1.3354	38°	55.8	53.4	1.70	1.86	1.68	1.86
		50°	100	100				
		60°	159	159				

30°C

Conc. Wt. %	n	θ	$\Delta\omega_1$, Hz	$\Delta\omega_2$, Hz	$D_{13} \times 10^8$ cm ² /sec	$D_{14} \times 10^8$ cm ² /sec	$D_{23} \times 10^8$ cm ² /sec	$D_{24} \times 10^8$ cm ² /sec
0.50	1.3356	38°	75.8	76.8	1.84	1.61	1.84	1.60
		50°	108	108				
		60°	137	136				
0.20	1.3352	38°	59.0	55.8	1.59	1.57	1.51	1.50
		50°	93.8	88.8				
		60°	134	128				
0.10	1.3350	38°	45.3	38.6	1.31	1.34	1.22	1.33
		50°	79.7	76.5				
		60°	113	111.4				
0.05	1.3350	38°	45.4	42.3	1.33	1.38	1.26	1.33
		50°	81.8	76.4				
		60°	116	112				

35°C

Conc. Wt. %	n	θ	$\Delta\omega_1$, Hz	$\Delta\omega_2$, Hz	$D_{13} \times 10^8$ cm ² /sec	$D_{14} \times 10^8$ cm ² /sec	$D_{23} \times 10^8$ cm ² /sec	$D_{24} \times 10^8$ cm ² /sec
0.50	1.3347	38°	68.0	67.6	1.82	1.71	1.85	1.79
		50°	113	114				
		60°	143	150				
0.20	1.3342	38°	59.9	55.3	1.64	1.56	1.56	1.54
		50°	103	96.9				
		60°	130	129				
0.10	1.3342	38°	48.5	42.1	1.39	1.39	1.30	1.36
		50°	86.5	82.7				
		60°	116	113				
0.05	1.3341	38°	51.8	46.7	1.47	1.43	1.40	1.44
		50°	94.6	89.8				
		60°	118	119				

APPENDIX B

Alignment of Light Receiving System

(See Figure 9)

The following procedure is to be carried out with the shutter closed on the photomultiplier tube.

1. Remove L_1 , L_2 , P_4 from the optical rail and take out L. P. and P_3 . Remove the pinholes, P_1 and P_2 , from their mounts on the platform. Rotate the platform to 0° .
2. Turn on the sighting laser, S. L.
3. Put two pinholes with exactly the same height on the optical rail in the positions occupied previously by L_1 and P_4 .
4. Adjust the sighting laser so that its beam passes through the exact centers of the two pinholes. This laser beam is now parallel to the optical rail.
5. Replace L. P. and P_3 . Adjust the aperture of P_3 to its narrowest setting and center it in the laser beam.
6. Remove the pinhole closest to the sighting laser and replace it with L_1 .

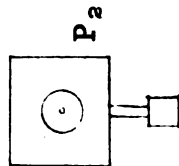
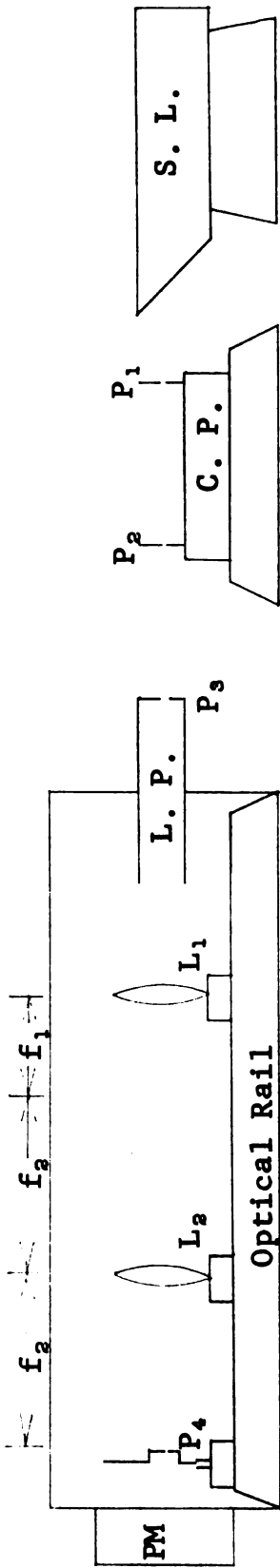


Figure 9.--Light receiving system, side view

- PM = Photomultiplier tube
- P₁, P₂, P₃, P₄ = Adjustable pinholes
- L₁, L₂, L₃ = Lenses with focal lengths f_1 , f_2
- S. L. = Sighting laser
- L. P. = Light pipe on which P₃ is mounted
- C. P. = Cell platform

7. Adjust the horizontal, vertical, and rotational position of L_1 so that the laser beam goes through the center of the remaining pinhole.
8. Put L_2 in position and adjust it in the same manner used for L_1 (Step 7).
9. Put P_4 in place on the rail and adjust its vertical and horizontal position so the laser beam passes through it. Adjust the size of the aperture so that it is small enough to cut off all diffraction patterns, but large enough to let the main beam go through untouched.
10. Return P_1 and P_2 to their mounts and adjust their horizontal and vertical positions so they are centered in the laser beam.

Note: The relative positions of L_1 , L_2 , and P_4 are determined by the focal lengths of the lenses, as shown in Figure 9. P_4 should be as close to PM as possible.

APPENDIX C

Adjustment of the Scattering Angle

(See Figure 10)

1. Remove the temperature control cell and the sample cell.
2. Rotate the cell platform to the desired angle.
3. Adjust the laser and the mirror so the light beam passes through the center of the two pinholes, P_1 and P_2 .
4. Remove the pinholes from their mounts and replace the temperature control cell.
5. Place the sample cell in the temperature control cell and center it in the incident beam. The cell is centered when the back reflection from the cell is superimposed on the incident beam.

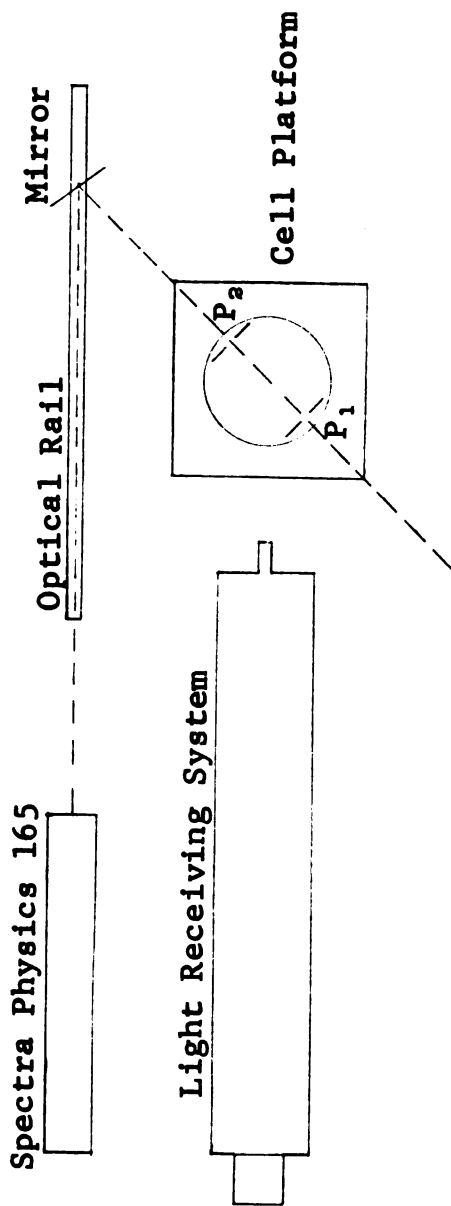


Figure 10.--Close-up of the homodyne system

P_1 , P_a Removeable pinholes

MICHIGAN STATE UNIVERSITY LIBRARIES



3 1293 03146 1563